Appl Biochem Biotechnol (2014) 173:1003–1010
DOI 10.1007/s12010-014-0911-5

Synthesis of Nano-hydroxyapatite via Microbial Method and Its Characterization

Xin Wang · Chunxiang Qian · Xiaoniu Yu

Received: 13 December 2013 / Accepted: 7 April 2014 /
Published online: 22 April 2014

Abstract Nanoparticles of hydroxyapatite were successfully synthesized by microbial method at ambient temperature and pressure, using calcium chloride and specific substrate as reactants. The compositional and morphological properties of products of the syntheses were studied by means of X-ray diffraction (XRD), Fourier transform infrared (FTIR) spectroscopy, scanning electron microscopy (SEM), transmission electron microscopy (TEM), and thermogravimetric analysis (TGA). The characterization data obtained showed that the phase composition, functional groups, and surface morphology of samples obtained by microbial method were mainly similar to that by chemical precipitation method. The hydroxyapatite powder was shown to be nanometer-grade in size and sphere-like in shape.

Keywords Microbial method · Hydroxyapatite · Mineralization · Nanoparticle · Characterization

Introduction

Biological mineralization as a common phenomenon in nature is a process of solid phases of various materials with special advanced structures assembled in biological systems. During this process, organic macromolecules and inorganic ions interact in the interphase which enables the biogenic mineral to have a special multiscale structure and assembly regulating inorganic mineral face separated from the molecular level.

Hydroxyapatite ($Ca_{10}(PO_4)_6(OH)_2$), abbreviated as "HA," is one of the most attractive ceramic materials for vertebrate and dental implant applications due to their compositional and biological similarity to native hard tissues [1, 2]. It can be synthesized by a variety of methods including conventional ones, such as hydrothermal [3, 4], sol-gel [5, 6], hydrolysis [7, 8], solid-state reaction [9, 10], coprecipitation [11, 12], and so on. However, these methods are relatively complex or indispensable harsh reaction conditions. Taking biological mineralization into consideration, HA is likely to be prepared via microbial activity and microorganisms, just like microbe-induced calcite precipitation (MICP), which has been widely studied and

X. Wang · C. Qian · X. Yu
School of Material Science and Engineering, Southeast University, 211189 Nanjing, China

X. Wang · C. Qian (✉) · X. Yu
Research Institute of Green Construction Materials, 211189 Nanjing, China
e-mail: cxqian@seu.edu.cn

successfully applied to some actual engineering fields [13–16]. To the author's knowledge, this microbial method has not been proposed or adopted yet by other researchers to synthesize hydroxyapatite.

In this paper, an appropriate phosphate mineralization bacteria has been selected, for example, for the use of the enzymatic effect in the growth and reproduction process to decompose a specific substrate and the addition of Ca^{2+} to form ($Ca_{10}(PO_4)_6(OH)_2$) in a certain time, which has a nano-level spherical cluster on its surface. In addition, the morphology, structure, and thermal decomposition properties of the hydroxyapatite precipitates were characterized by scanning electron microscopy (SEM), transmission electron microscopy (TEM), Fourier transform infrared (FTIR), X-ray diffraction (XRD), and differential scanning calorimetry-thermogravimetry (DSC-TG).

Experimental and Methods

Materials

All chemicals were of analytical grade and used without further purification. The bacterium was selected to investigate microbe-induced phosphate precipitation. A microbial culture with optical density (at 600 nm of wavelength) value of 1.0 and enzyme activity value of 0.5 mmol/(L min) was used in this study. Cultivation of the organism was conducted in beef extract peptone culture (3 g of yeast extract and 5 g of peptone were dissolved in deionized water to 1 L, and the pH value was adjusted to about 7.0) at 30 °C for 24 h. Then, the harvested microorganisms were kept in a refrigerator at 4 °C for stock prior to use. The concentrations of the substrate and calcium ion solution were 50 and 100 mmol L^{-1}, respectively.

The instruments used were listed as follows: Sirion field emission scanning electron microscope (FEI Company, Netherlands), transmission electron microscope (FEI Company, Netherlands), Nicolet-5700 Fourier infrared spectroscope (American Nicolet Corporation, USA), D8-Discover X-ray diffractometer (Bruker Company, Germany), and STA449 F3 Thermogravimetry analyzer (NETZSCH Company, Germany).

Chemical Method

A stoichiometric amount of aqueous solution of calcium nitrate tetrahydrate ($Ca(NO_3)_2{\cdot}4H_2O$, 0.5 mol L^{-1}) was used and mixed with an aqueous solution of diammonium hydrogen phosphate ($(NH_4)_2HPO_4$, 0.3 mol L^{-1}) with the molar ratio of 10:6 through a peristaltic pump, and the reaction was carried out in the stirred beaker at 300 rpm and 90 °C for 1 h. It is necessary to ensure that the pH of reaction system should be around 10.5 during the reaction, which is always adjusted by ammonia water ($NH_3{\cdot}H_2O$, 25 %). After being aged for 12 h, the products were filtrated and washed three times with deionized water and ethanol and then dried at 60 °C for 12 h. The chemical samples were collected.

Microbial Method

A given amount of the substrate was completely dissolved in 150 mL of deionized water to the concentrations of 150 mmol·L^{-1}, and its pH value was adjusted to about 9.0 using 0.1 mol L^{-1} NaOH aqueous solution; 450 mL of 100 mmol L^{-1} $CaCl_2$ solutions was also prepared prior to use. One liter of liquid medium was prepared using deionized water, 3 g of yeast extract, and 5 g of peptone and was shaken to obtain a clear solution which was then adjusted to a pH value

of about 7.0 using 0.1 mol L^{-1} NaOH aqueous solution. One hundred milliliters of the ready medium was added to a 250-mL flask bottle and sterilized. The liquid media was made in triplicate and kept in three bottles. Next, 5 mL of liquid strains was added to each bottle and cultivated in the oscillation incubator (170 r·min^{-1}) at the temperature of 30 °C for 24 h. According to abovementioned methods, we were likely to obtain the bacterial liquid with an optical density (at 600 nm of wavelength) value of 1.0 and enzyme activity value of 0.5 mmol L^{-1} min^{-1}.

The substrate solution was made in triplicate and poured into each bottle containing the bacterial liquid, respectively. After the reaction for 2 h, 150 mL of 100 mmol L^{-1} calcium chloride was introduced. After stirring for 10 min, each bottle was allowed to stand for 12 h. The above experiments were performed at an ambient temperature of 30±2 °C. As the same procedure mentioned in the "Chemical Method" section, the microbial sample was also obtained.

Analysis of Precipitation

The crystal structure of the product was analyzed by D8-Discover XRD, which used a tube voltage of 40 kV and current of 40 mA with Cu K_α radiation of 1.5406 Å. The scanning angle range was from 10° to 60° 2θ with the step at 0.2 s/step. The average crystallite size of the precipitates was estimated by using the simple Scherrer's equation [17]:

$$D = \frac{k\lambda}{\beta_{1/2} cos\theta}$$

where D is the size in angstrom measured using certain reflection, k the shape factor equal to 0.89, λ the wavelength of X-rays equal to 1.5406 Å, θ the diffraction angle for the selected reflection, and $\beta_{1/2}$ is defined as the diffraction peak width at half height, expressed in radians.

SEM (FEI Company, Netherlands) with a GENESIS 60S energy dispersive X-ray spectroscope (EDS) spectroscopy system with magnification from 10,000 to 100,000 was used to observe the morphology and to measure the elemental compositions of the precipitation. The accelerating voltage and spot size of the secondary electron detector were 20 kV and 4.0, respectively.

TEM (FEI Company, Netherlands) was carried out to confirm the SEM analysis, and the accelerating voltage and spot resolution were 400 kV and 0.12 nm, respectively.

The IR spectrum of the product was recorded using a Nicolet 5700 spectrometer by KBr pellet technique with the resolution of 4 cm^{-1} and scanning the product for 20 times in the range of 4,000~500 cm^{-1}.

The thermal properties of the products were investigated by STA449 F3 thermogravimetric analyzer in nitrogen atmosphere with the elevated temperature range of room temperature to 1,000 °C at a rate of 10 °C min^{-1}.

Results and Discussion

XRD Analysis

The XRD patterns of hydroxyapatite precipitate induced in the abovementioned bacterial liquid is shown in Fig. 1. Figure 1 shows that all the peaks are in a good agreement with standard (JCPDS card number 09-0432). The two products are characterized by a crystalline

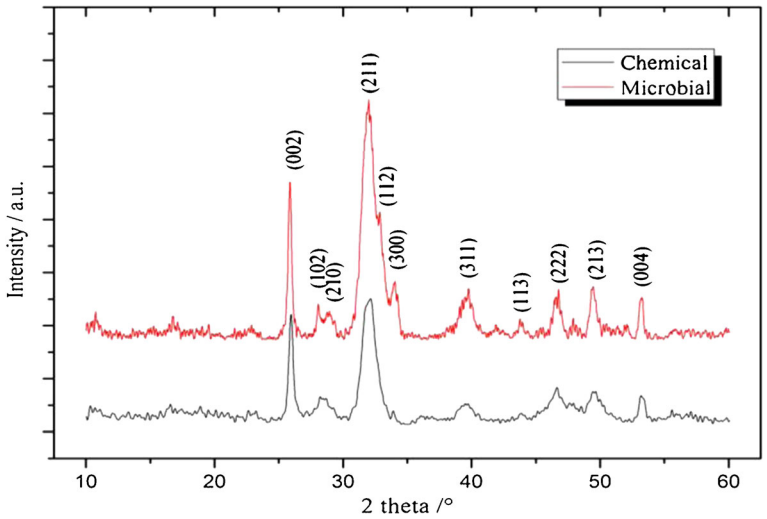

Fig. 1 XRD patterns of hydroxyapatite precipitate obtained by chemical and microbial methods

structure and a low crystallinity, as evidenced by XRD patterns with relatively broad and low-intensity XRD peaks, which are marked by triplets or broad, intense diffraction band ranging from 31.82° to 34.07° 2θ and an individual intensive peak at 25.89° 2θ characteristic to an apatite phase [18]. It is well known that a lower synthetic temperature decreases the resultant HA crystallinity, and microbial activity and microorganism also have an effect on crystal growth. Compared with the diffraction peak of the chemical product, there is no evident difference in their diffraction peak position but the intensity. Table 1 shows the average crystallite size of the precipitates estimated by applying Scherrer's formula. It is suggested that hydroxyapatite particles obtained both by the chemical and microbial methods are of nanometer grade [19].

FTIR Analysis

In order to obtain complementary information in the presence of HA, FTIR analysis was also conducted. Figure 2 illustrates FTIR results obtained for different samples (chemical and microbial), in the spectral region from 500 to 4,000 cm^{-1}.

The FTIR spectra of HA prepared by both methods show a very similar structure. For the microbial product, functional groups present are confirmed in Fig. 2. The characteristic bands for PO_4^{3-} appear at 553, 602, 1,028, and 1,102 cm^{-1} [20–22]. The traces at 553 and 602 cm^{-1} are attributed to the υ2 bending vibration. The bands at 1,028 and 1,102 cm^{-1} respond to the

Table 1 The estimated value of the average crystallite size of the precipitates

Sample	θ (deg)	$\beta_{1/2}$ (deg)	D (nm)
Microbial group	12.97	0.406	19.86
Chemical group	12.94	0.470	17.15

The values of θ and $\beta_{1/2}$ are obtain using selected reflection (0 0 2)

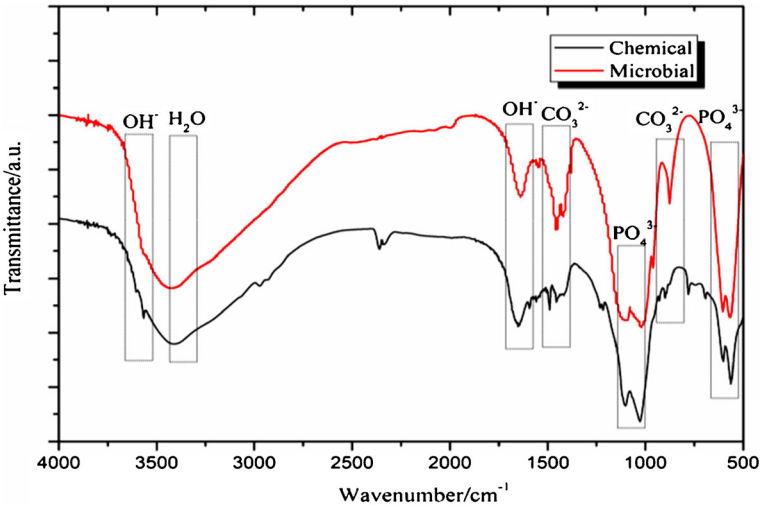

Fig. 2 FTIR spectra of hydroxyapatite precipitate via chemical and microbial methods

υ3 vibrations of PO_4^{3-} ions. For the OH– group of sample, peak positions are at 1,651 and 3,575 cm^{-1}. The wide band of H_2O at around 3,412 cm^{-1} can be observed in the FTIR analysis of the samples. Adsorption bands available at 874, 1,419, and 1,455 cm^{-1} correspond to carbonate adsorption [23]. A possible explanation for this phenomenon is that atmospheric CO_2 might have been absorbed by the sample when tested.

Electron Microscopic Analysis

SEM and TEM photographs of hydroxyapatite samples obtained by the two methods are shown in Fig. 3. As SEM images show, the overall evaluation of the morphology of the samples indicates a suitable and uniform distribution of small particles within the large agglomerates of HA nano-composites, with a particle size in the range of 20~40 nm. By comparison, it is obviously found that a sphere-like grain prepared by the microbial method is slightly larger in size than that of the chemical method. The TEM micrograph of nanoparticles confirms the SEM analysis. The organic matrix secreted by the microorganism could have an effect on the crystal nucleation and growth because the organic matter or bio-protein was able to induce inorganic mineral precipitation on the interface between the organic matter and solution as template [24].

TG/DSC Analysis

The thermal stability of hydroxyapatite samples was determined by thermogravimetric analysis in air atmosphere as shown in Fig. 4. There is no evident difference between curves of the chemical product and microbial ones in tendency.

For both the chemical and microbial samples, there are two obvious weight loss behaviors, which correspond to respective thermal changes of DSC curves. The first DSC peak occurs at around 80 °C, and the corresponding weight loss is respectively 6.86 and 8.37 %, which may result from the volatile-endothermic residual impregnate, such as deionized water and ethanol.

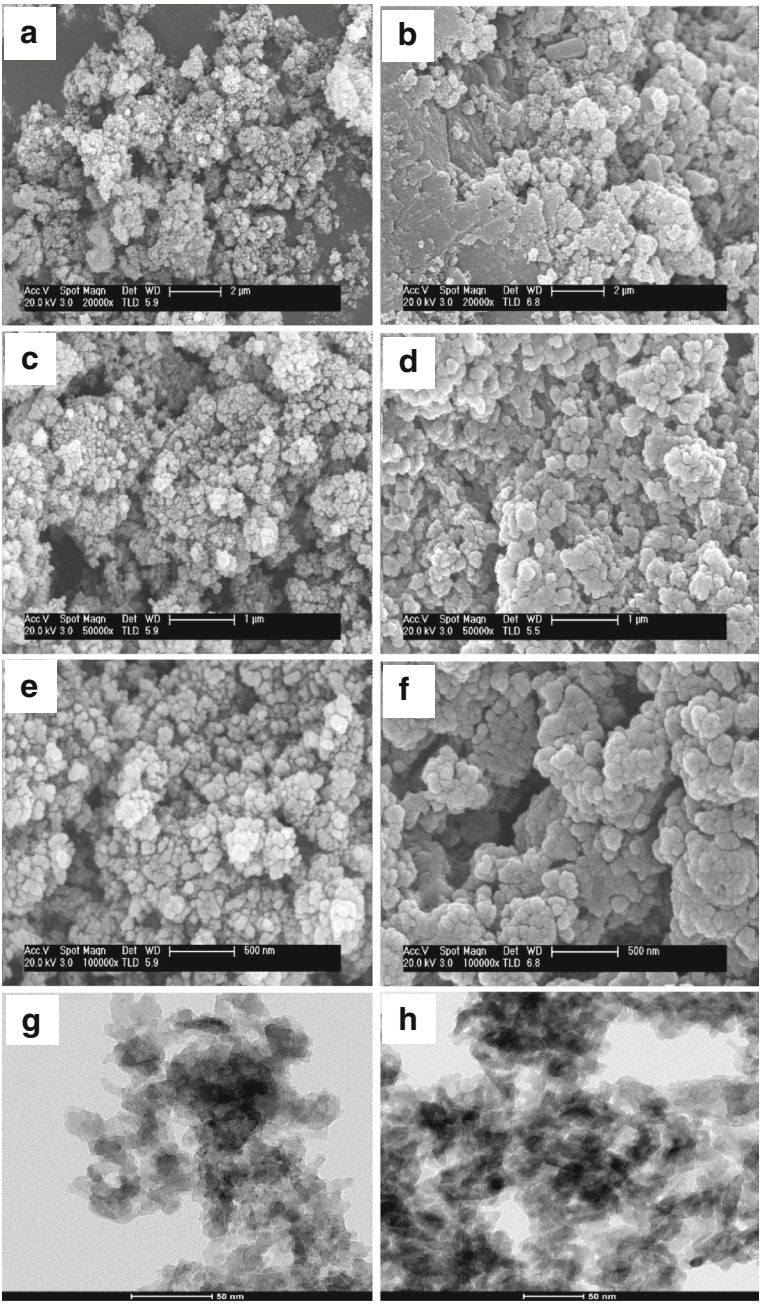

Fig. 3 SEM and TEM images of hydroxyapatite samples via chemical (**a**, **c**, **e**, **g**) and microbial (**b**, **d**, **f**, **h**) methods

For the microbial sample, the second peak at around 295 °C corresponds to organic decarbonization, oxidization, and burning, which bring about 13.81 % of weight losses.

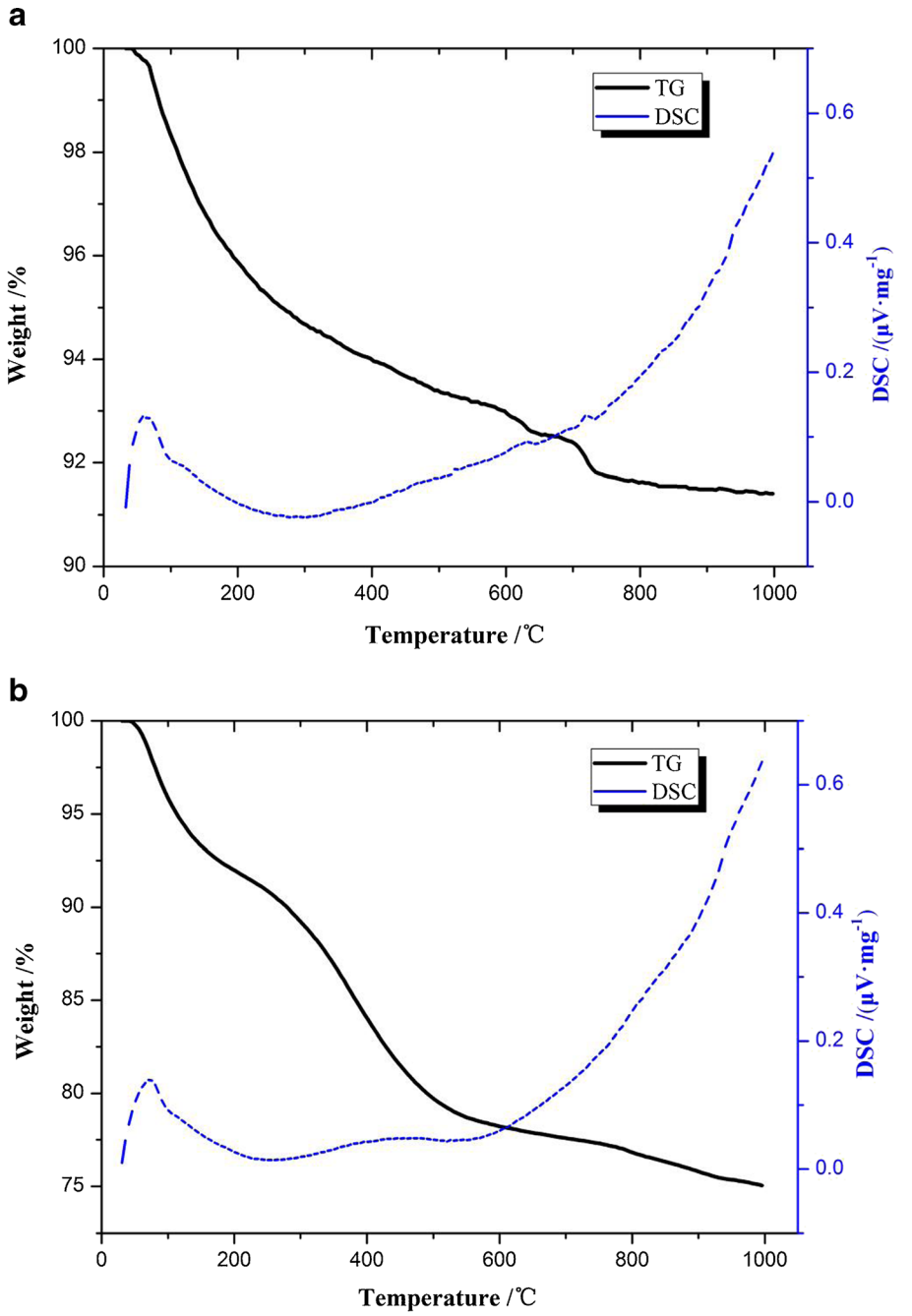

Fig. 4 Thermal analysis curves of hydroxyapatite precipitate via chemical (**a**) and microbial (**b**) methods

There is no significant weight loss over 750 °C, which indicates that hydroxyapatite basically reaches a stable state.

Conclusions

In this study, we conducted a fundamental laboratory experiment on the synthesis of hydroxyapatite powder by microbial method at ambient temperature and pressure conditions, which has not been proposed by other researchers yet. Compared with the hydroxyapatite sample prepared by conventional chemical method, it shows similar a property of production to a chemical product, or superior to it to a certain extent. XRD diffraction graph and FTIR spectra confirmed the structure of hydroxyapatite, and SEM morphology analysis shows that the hydroxyapatite powder has a sphere-like shape and a diameter of dozens of nanometer. In a word, this microbial method has obvious advantages over the conventional method, such as more moderate reaction condition, simple to operate, and so on. Furthermore, the peculiar advantages of microorganisms, such as high reproducibility and low cost, provide the possibility for some engineering applications.

Acknowledgments This work was supported by the National Nature Science Foundation of China (Grant No. 51372038).

References

1. Que, W., Khor, K. A., Xu, J. L., & Yu, L. G. (2008). *Journal of the European Ceramic Society, 28*, 3083–3090.
2. Enayati-Jazi, M., Solati-Hashjin, M., Nemati, A., & Bakhshi, F. (2012). *Superlattices and Microstructures, 51*, 877–885.
3. Jinawath, S., Polchai, D., & Yoshimura, M. (2002). *Materials Science and Engineering: C, 22*, 35–39.
4. Suchanek, W. L., Shuk, P., Byrappa, K., Riman, R. E., TenHuisen, K. S., & Janas, V. F. (2002). *Biomaterials, 23*, 699–710.
5. Liu, D. M., Troczynski, T., & Yseng, W. J. (2001). *Biomaterials, 22*, 1721–1730.
6. Masuda, Y., Matubara, K., & Sakka, S. (1990). *Journal of the Ceramic Society of Japan, 98*, 1255–1266.
7. Yoon, S. Y., Park, Y. M., Park, S. S., Stevens, R., & Park, H. C. (2005). *Materials Chemistry and Physics, 91*, 48–53.
8. Monma, H. T., & Kamiya. (1987). *Journal of Materials Science, 22*, 4247–4250.
9. Kalita, S. J., Bhardwaj, A., & Bhatt, H. A. (2007). *Materials Science and Engineering: C, 27*, 441–449.
10. Rao, R. R., Roopa, H. N., & Kannan, T. S. (1997). *Journal of Materials Science: Materials in Medicine, 8*, 511–518.
11. Correia, R. N., Magalhaes, M. C. F., Marques, P. A. A. P., & Senos, A. M. R. (1996). *Journal of Materials Science: Materials in Medicine, 7*, 501–505.
12. Wu, Y. S., Lee, Y. H., & Chang, H. C. (2009). *Materials Science and Engineering: C, 29*, 237–241.
13. Whiffin, V. S. (2004). PhD thesis, Murdoch University, Australia.
14. Chaturvedi, S., Chandra, R., & Rai, V. (2006). *Ecological Engineering, 27*, 202–207.
15. De, M. W., De, B. N., & Verstraete, W. (2010). *Ecological Engineering, 36*, 118–136.
16. Ivanov, V., & Chu, J. (2008). *Reviews in Environmental Science and Biotechnology, 7*, 139–153.
17. Mostafa, N. Y. (2005). *Materials Chemistry and Physics, 94*, 333–341.
18. Stipniece, L., Salma-Ancane, K., Borodajenko, N., Sokolova, M., Jakovlevs, D., & Berzina-Cimdina, L. (2014). *Ceramics International, 40*, 3261–3267.
19. Salimi, M. N., & Anuar, A. (2013). *Procedia Engineering, 53*, 192–196.
20. Webster, T. J., Siegel, R. W., & Bizios, R. (1999). *Biomaterials, 20*, 1221–1227.
21. Pushpakanth, S., Srinivasan, B., Sreedhar, B., & Sastry, T. P. (2008). *Materials Chemistry & Physics, 107*, 492–498.
22. Manjubala, I., Woesz, A., Pilz, C., Rumpler, M., Fratzl-Zelman, N., Roschger, P., et al. (2005). *Journal of Materials Science: Materials in Medicine, 16*, 1111–1119.
23. Jokic, B., Mitric, M., Radmilovic, V., Drmanic, S., Petrovic, R., & Janackovic, D. (2011). *Ceramics International, 37*, 167–173.
24. Weiner, S., & Dove, P. M. (2003). *Reviews in Mineralogy and Geochemistry, 54*, 1–29.